Geo-Mar Lett (2017) 37:593–606
DOI 10.1007/s00367-017-0514-6

ORIGINAL

Regional distribution patterns of chemical parameters in surface sediments of the south-western Baltic Sea and their possible causes

T. Leipe[1] · M. Naumann[1] · F. Tauber[1] · H. Radtke[1] · R. Friedland[1] · A. Hiller[1] · H. W. Arz[1]

Received: 6 February 2017 / Accepted: 7 June 2017 / Published online: 15 June 2017

Abstract This study presents selected results of a sediment geochemical mapping program of German territorial waters in the south-western Baltic Sea. The field work was conducted mainly during the early 2000s. Due to the strong variability of sediment types in the study area, it was decided to separate and analyse the fine fraction (<63 μm, mud) from more than 600 surficial samples, combined with recalculations for the bulk sediment. For the contents of total organic carbon (TOC) and selected elements (P, Hg), the regional distribution maps show strong differences between the analysed fine fraction and the recalculated total sediment. Seeing that mud contents vary strongly between 0 and 100%, this can be explained by the well-known grain-size effect. To avoid (or at least minimise) this effect, further interpretations were based on the data for the fine fraction alone. Lateral transport from the large Oder River estuary combined with high abundances and activities of benthic fauna on the shallow-water Oder Bank (well sorted fine sand) could be some main causes for hotspots identified in the fine-fraction element distribution. The regional pattern of primary production as the main driver of nutrient element fixation (C, N, P, Si) was found to be only weakly correlated with, for example, the TOC distribution in the fine fraction. This implies that, besides surface sediment dynamics, local conditions (e.g. benthic secondary production) also have strong impacts. To the best of the authors' knowledge, there is no comparable study with geochemical analyses of the fine fraction of marine sediments to this extent (13,600 km^2) and coverage (between 600 and 800 data points) in the Baltic Sea. This aspect proved pivotal in confidently pinpointing geochemical "anomalies" in surface sediments of the south-western Baltic Sea.

✉ T. Leipe
thomas.leipe@io-warnemuende.de

[1] Leibniz Institute for Baltic Sea Research Warnemünde (IOW), Seestraße 15, 18119 Rostock, Germany

Introduction

Sediment geochemical data are crucial for assessing the function of sediments in the ecosystem. The German research project "SECOS" (The Service of Sediments in German Coastal Seas) started in 2013 and included a sediment geochemical mapping as one important tool for later compilation of a complete "Baltic Sea Atlas", a related database to be used for GIS applications. For some larger parts of the Baltic Sea, sediment geochemistry has already been studied during past decades and sediment geochemical maps have been published by, for example, Emelyanov et al. (1995; Bornholm Basin), Borg and Jonsson (1996; Baltic Sea, trace metals), Emelyanov (2002; Gdansk Basin), Uscinowicz (2011; Polish Baltic Sea), Vallius (2007; Gulf of Finland), and Emelyanov (2012; Gotland Basin).

Modern web-GIS based maps are published at the homepages of the geological surveys of Sweden and Finland. The geochemical maps cover only the land areas and, unfortunately, not the marine areas. Moreover, most earlier geochemical mapping exercises were performed on bulk sediments, rather than on specific grain-size fractions.

For the present study in the south-western Baltic Sea, it was decided to separate the fine fraction (<63 μm, mud) before elemental analyses to search for geochemical signatures, thereby at least minimising the grain-size effect. Accompanied by the large spatial extent (13,600 km^2) and coverage (between 600 and 800 data points) of data collection, this aspect proved pivotal in confidently earmarking geochemical "anomalies" in these surface sediments.

Regional setting

The present study and most of the investigated surface sediment samples are based on the German Baltic Sea floor mapping published in 2012 by the Federal agency of Shipping and Hydrography (BSH; Tauber 2012; nine sheets, scale 1:100,000). From the grain-size data of these samples, a classification resulted in the definition of six major sediment types for the south-western Baltic Sea (Fig. 1, Table 1).

The German sector of the Baltic Sea is characterised by large and mostly sandy shallow-water areas. Partly gravelly, so-called lag sediments occur in wave-exposed areas from where fine-grained material is removed (e.g. coastal zone, Falster-Rügen Bank and Oder Bank) to be deposited at greater depths in the form of organic-rich mud (e.g. Mecklenburg Bay and Arkona Basin). For land-derived material input, mainly the Oder River and its estuary in the eastern part of the study area is important. Some of the relevant sub-regions and geographical names are included in Fig. 2.

Materials and methods

Sampling and sample treatment

Surface sediments (0–2 cm) were collected by grab sampler (sand, hard ground), box-corer or multi-corer (soft sediment) during several cruises in the period 2000–2013. The field work was performed in blocks designed for the different sub-areas of the German territorial waters, and dependent on ship time. The samples for each sub-area were collected within ca. 2 years. The sample locations are displayed in Fig. 2. The selection of samples for the present investigations took into account a regular coverage of the whole area and a sufficient representation of each of the major sediment types. Complete grain-size data (obtained by sieve- and laser-based analyses) were already available for all the samples (see Tauber 2012) before the geochemical analyses of the present study.

The fine fraction (<63 μm) of the bulk sediment was separated by means of a plastic mesh (to avoid metal contamination) with a mesh size of 63 μm. The original sediment samples were suspended in fresh water to dilute the salt, followed by ultrasonic treatment to destroy aggregates before sieving. The separated fine-fraction suspension was collected in glass beakers, centrifuged to remove the water (and salt) and then freeze-dried for later analyses.

The decision to separate the fine fraction for geochemical analyses follows the recommendation by Perttilä and Brügmann in 1992, developed and later used for sediment environmental monitoring programs (HELCOM 2007). The advantages of this method are that comparable results from different regions and sediment types are achieved, while grain-size effects are excluded (or at least minimised). Additionally, it avoids analytical problems at the detection limit for coarser samples (sand). The present study is the first to employ this method for such a large sector (13,600 km^2) and data base (600–800 data points) for the Baltic Sea.

To make the present results comparable with former sediment geochemical mappings of other regions in the Baltic Sea, a recalculation of the element contents of the fine fraction "back" to the original bulk samples was done. Thus, the element contents of the bulk sediment were calculated from the fine-fraction analysis by proportional numerical "dilution" with the coarser part of the samples (weight% >63 μm), which was measured and available for all the samples. This approach seems acceptable if the elements of interest are concentrated (enriched) mostly in the fine fraction, rather than in the coarse fraction. The approach was successfully verified based on a

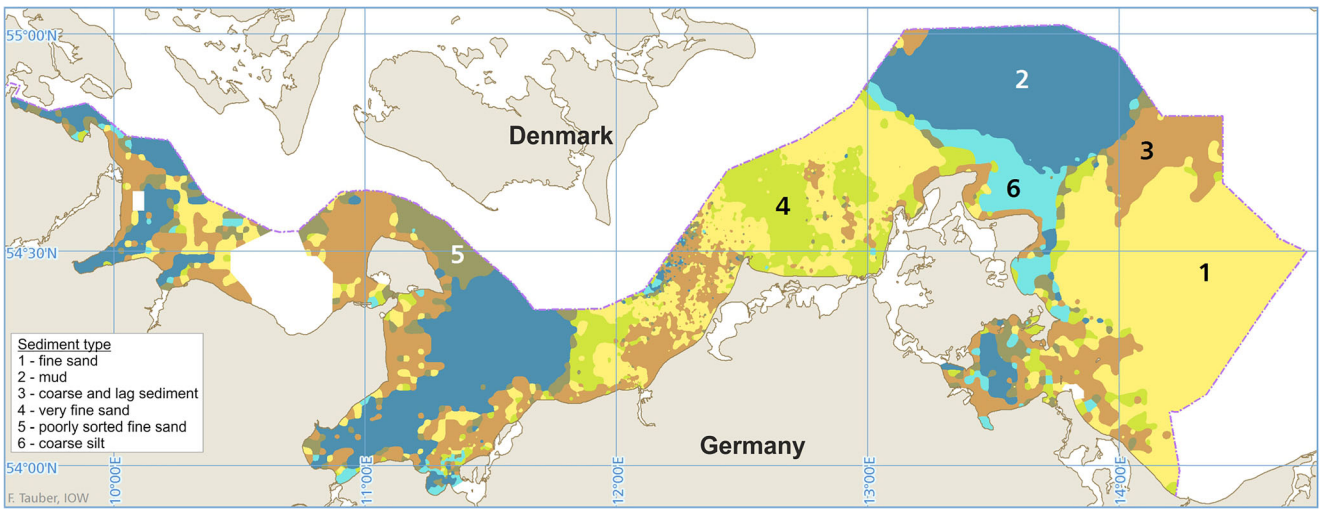

Fig. 1 Distribution map of major sediment types in the German Baltic Sea (see also Table 1). The blank sector in the western part of the study area (3% of total area) could not be sampled because it represented a restricted military zone

Table 1 The six major sediment types characterising the German Baltic Sea floor (cf. also Fig. 1)

No.	Sediment type	Median (μm)	Sorting (phi)	Type locality	Area (km^2)	Area (%)	Colour in Fig. 1
1	Fine sand	200	0.35	Oder Bank	4,541	32	Yellow
2	Mud	10	1.9	Arkona Basin	3,603	25	Dark blue
3	Coarse and lag sediment	550	0.9	Adlergrund	2,814	20	Brown
4	Very fine sand	120	0.4	N of Zingst Penin.	1,330	9	Light green
5	Poorly sorted fine sand	100	2.1	Fehmarnbelt	808	6	Dark green
6	Coarse silt	50	1	Tromper Wiek	637	5	Light blue

selected subset of samples. For all elements evaluated here, more than 90% of the total element contents could be accounted for by the fine fraction.

Geochemical analyses

Total carbon (TC), N and S were measured directly on dry samples using a Euro EA from Hekatech; and a EA 1110 CHN from CE-Instruments (GC-based methods). Total inorganic carbon (TIC) was determined directly by H_3PO_4 removal of carbonates with a Multi EA 4000 (IR method) from Analytic Jena. Total organic carbon (TOC) was then calculated as TOC=TC–TIC.

A DMA 80 from Milestone Lab.-Systems was used for direct Hg analyses, heating the sample Hg in a gold trap, heating again, and measuring by AAS. Biogenic opal (SiO_2) was determined after basic extraction: 50 mg of the dry sample was treated with 100 ml 1M NaOH for 40 min at 80 °C in shaking steel backers. The resulting suspensions were then centrifuged, filtrated, and prepared for Si analysis with ICP-OES. The method was developed and modified as proposed by Müller and Schneider (1993), and quality assurance was tested by including standard material from Conley (1998).

Total P and the elements As, Cr, Cu, Fe, Mn, Pb and Zn were analysed after 1N HCl extraction from dry samples after burning for 3 h at 550 °C by ICP-OES (iCAP 7000) and ICP-MS (iCAP Q), both from Thermo Scientific. This ash-extraction method was chosen because it is much easier to handle for large sample amounts compared to the total digestion methods, and it allows the detection of the majority of the element contents in relation to total digestion. Validation of the method is based on analyses of 26 samples from the present study area and two different standards using a total digestion method (strong acid mixture, and pressure bomb). For P

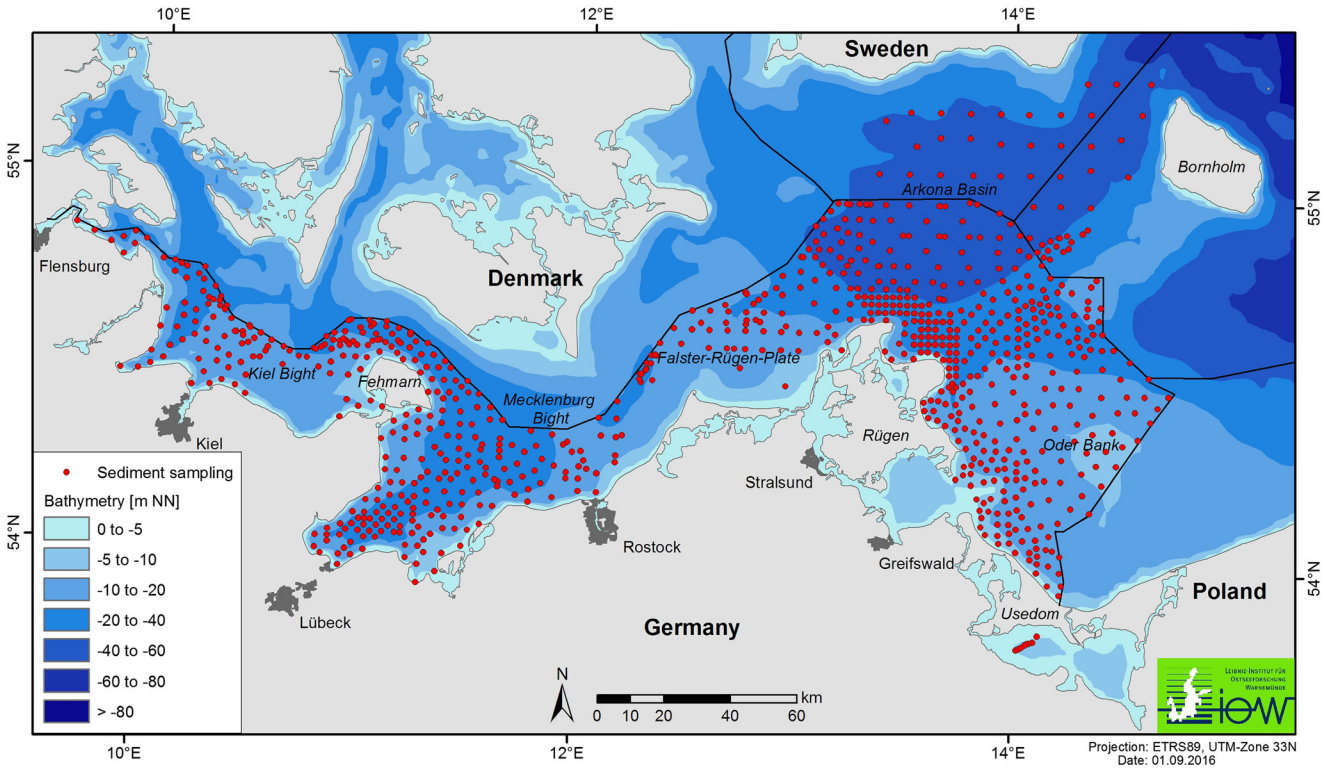

Fig. 2 Surficial sediment sampling locations and water depths (bathymetry) of the western Baltic Sea

(this element was the main reason for choosing the ash-extraction method), there is a linear regression of 1.043 x with R^2=0.979 and a recovery of 98% ash P from total P. For the other elements, the recovery is Fe: 74%; Mn: 73%; Cr: 65%; Cu: 95%; Pb: 91%; Zn: 92%; As: 89%. Table 2 gives an overview of the analytical methods and quality control.

GIS analysis and map construction

To construct area-wide maps of geochemical parameters, it is necessary to transfer the spatially irregularly distributed data points of laboratory analyses into regular grids. In a first step, the geographic coordinates of the sampling stations given in the geodetic reference system WGS84 were transformed into Cartesian coordinates of the geodetic reference system ETRS89 (UTM zone 33N) by using standardised routines of the software ArcGIS version 10.2. On the basis of these metric coordinates, equidistant grids of 250 m cell size were interpolated in a second step with the software SURFER version 12. Gridding was done by the kriging method using a semi-variogram model. This geostatistical method describing the spatial variance of measurements calculates an experimental variogram, which shows the variance of data points according to their distances in a specified radius. On the basis of this graph a model function was derived, which was used for the interpolation process to enhance the quality of the approximation.

To fit a model function for each geochemical parameter, different parametrisations such as function types, search radius variations and direction controlled calculation were tested. The search radius controls the number of data points used for the interpolation of grid points. Large radii smoothen local structures such as basins and sand bars, whereas smaller ones show such structures in greater detail. The interpolation of all geochemical parameters was done with a maximum of 60 km to include large-scale structures like the Arkona Basin in the north-eastern part of the investigation area in the spanned search radius. Larger radii lead to unwanted smoothing. Direction controlled interpolation was tested by elliptic search fields in west–east and north–south orientations to describe possible transport regimes and fluxes in sediments. Only in sub-areas, like the Oder Bank in the eastern part of the study area, were improvements visible; for the study area as a whole, no consistent direction control could be identified. All final interpolations were done without direction controlled search fields.

As function types are linear, quadratic, spherical and Gaussian functions were used, depending on the experimental variogram of each geochemical parameter. In a final step, the interpolated grids were processed in ArcGIS to develop individual classifications and labelling. Root mean square errors were calculated for each map (Figs. 3, 4, 5, 6) and the corresponding grid, and found to be in acceptable ranges.

Modelling

To relate sediment composition to local ecosystem productivity, net primary production rates were derived from a model simulation using the GETM hydrodynamic model (Burchard and Bolding 2002; Klingbeil and Burchard 2013), to which the latest version of IOW's ecosystem model ERGOM (Radtke et al. 2012) was coupled via the Framework for Aquatic Biogeochemical Models (FABM; Bruggeman and Bolding 2014). In the present case, a setup with 600 m horizontal resolution and 40 vertically layers was used, as previously validated by Klingbeil et al. (2014) and Gräwe et al. (2015a), and which automatically adapts towards stratification (Hofmeister et al. 2010; Gräwe et al. 2015b). Nutrient load data for the different rivers were compiled from four different sources: the Baltic Environmental Database of the Baltic Nest Institute (http://nest.su.se/models/bed.htm), the data from HELCOM (2015), Lääne et al. (2002) and the

Table 2 Chemical analyses quality control

Element	Method	Standards	Precision	Recovery	Z scores[a]		
Hg (μg/kg)	DMA 80 (AAS)	BCR 142 R	6.4	104.2	1.1	–0.1	–0.6
N (%)	CHN (GC)	MBSS-1	4.1	102.1			
S (%)	CNS (GC)	MBSS-1	2.1	102.8			
TC (%)	CHN (GC)	MBSS-1	6.2	92.9			
TIC (%)	EA 4000 (IR)	CaCO3	3.8	96.4	0.1	–0.2	0.3
TOC (%)	Calc. by diff. TC–TIC	MBSS-1	6.6	95.3	0.3	0.6	0.6
Si-opal (%)	ICP-OES	Conley (1998)	2.2	103.2			
As (mg/kg)	ICP-MS	MESS-2	5.3	120.6	0.6	0.8	1.1
Cr (mg/kg)	ICP-MS	PACSS-1	6.3	85.8	1.5	–1.3	1.3
Cu (mg/kg)	ICP-MS	PACSS-1	10.1	104.2	–0.1	–0.1	–0.4
Fe (%)	ICP-OES	MESS-2	3.1	86.8	–0.1	0.4	–0.4
Mn (mg/kg)	ICP-OES	MESS-2	3.7	88.75	0.5	1.1	–0.1
P (%)	Photom. & ICP-OES	PACSS-1	0.7	101.3			
Pb (mg/kg)	ICP-MS	PACSS-1	11.2	101	0.3	0.5	–0.3
Zn (mg/kg)	ICP-MS	PACSS-1	3.4	92.1	0.4	0.4	0

[a] Z scores from QUASIMEME (metals in sediments, last rounds)

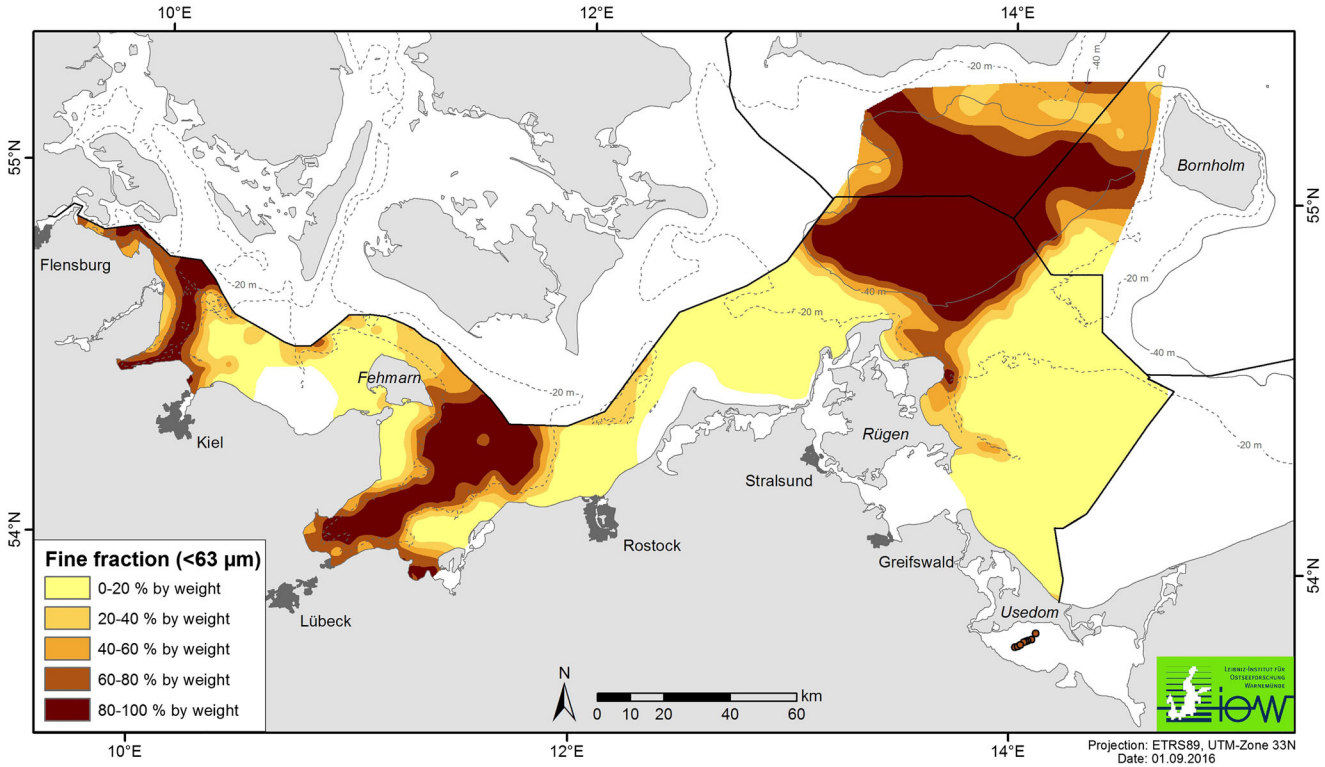

Fig. 3 Regional distribution of the fine fraction (<63 µm, weight% of total sediment). The fine fraction was separated for geochemical analyses

German environmental authorities. Three-hourly forecasts of the German Weather Service (DWD), created by the COSMO/EU model, were used as atmospheric forcing. Net primary production was calculated as the difference between phytoplankton gross carbon uptake and respiration.

For validation of model-based primary production, the modelled surface chlorophyll values were compared to satellite-derived estimates provided by the Copernicus website (marine.copernicus.eu), which are calculated from ocean colour measurements following an algorithm developed by Doerffer (2014). These daily estimates were derived from multi-satellite data via the BalAlg algorithm (Pitarch et al. 2016) and cover the complete modelled area and period. In a point-to-point comparison, the data show a correlation of only 49.6%. This is due to inability of the model to predict the exact location of meso-scale structures present in the 1 km spaced observations. If the chlorophyll concentrations are averaged over time (to analyse only the spatial variability), then the correlation coefficient rises to 75.5%.

Results

Altogether about 850 fine-fraction samples were analysed for TOC, TIC, N, S, Hg and biogenic opal (SiO_2) and, of these, about 600 samples were additionally analysed for As, Cr, Cu, Fe, Mn, P, Pb and Zn. All measured elements are reported as contents in relation to the dry weight of the sample material (mass per unit mass).

Table 3 gives an overview of statistical parameters of the analytical results. Table 4 shows a correlation matrix of the elements analysed in the fine sediment fraction. The regional distribution of the fine fraction is shown in Fig. 3 (cf. sediment types in Fig. 1: fine-grained mud in the basins, and coarse sediments in the shallower areas of banks, sand flats, and coastal zones). For the geochemical results, three selected constituents (TOC, P, Hg) are reported in Figs. 4, 5, and 6. Finally, the two scatter plots of Fig. 7 depict the correlation of primary production and chlorophyll a to the TOC contents of the fine fraction.

The fine fraction of sediments is generally considered to be the main carrier and "reactor" of environmentally relevant material fluxes and cycles because the coarse fraction commonly consists of chemically inert quartz grains, rock fragments and silicate minerals, as is the case in the present study area. The elements and other components analysed here can be allocated to three functional groups: (1) biogenically relevant (TOC, N, P, bio-opal), (2) at least partly redox-sensitive (Fe, Mn, P, S), and (3) strong anthropogenic impact (Hg, Pb, Cu, Zn, As). The carbonate content (TIC) of most samples was very low throughout the investigated area, and therefore can be considered as less important within the present context.

In these groups, the three selected constituents can be seen as representative of primary (and secondary)

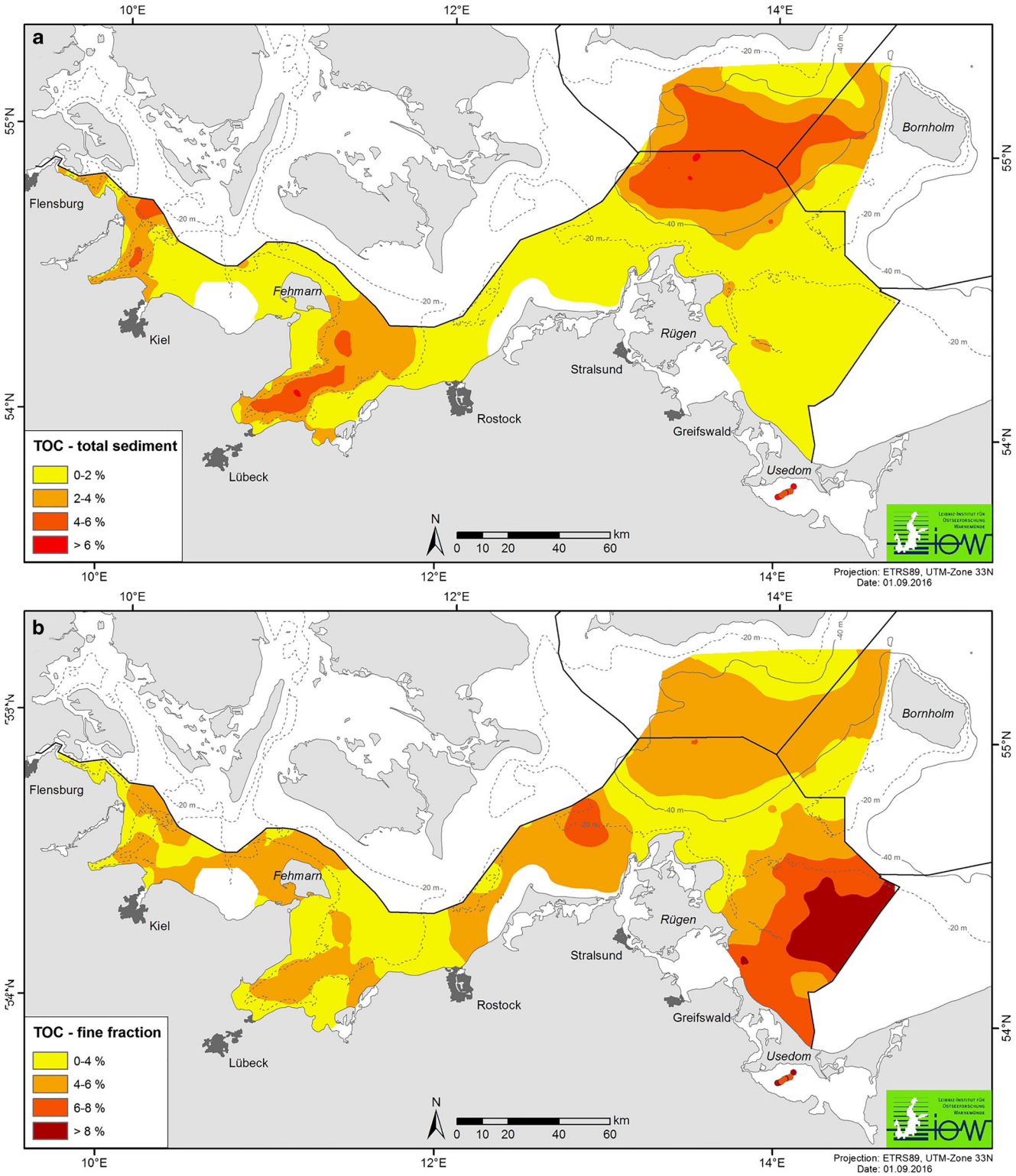

Fig. 4 Distribution of organic carbon (weight% TOC): **a** total sediment, **b** fine fraction. Note that the scales (legend) of the content ranges are different in **a** and **b**, which improves the visibility of the gradients

production (TOC, Fig. 4), eutrophication (P, Fig. 5), and anthropogenic impact (Hg, Fig. 6). In each of Figs. 4, 5 and 6, the top map shows the calculated content for the total (bulk) sediment, whereas the bottom map shows the distribution pattern for the analysed fine fraction. In order to better visualise the data and to improve the comparison of the spatial differences (patterns) in the maps, different scaling intervals were used for the total sediment and fine

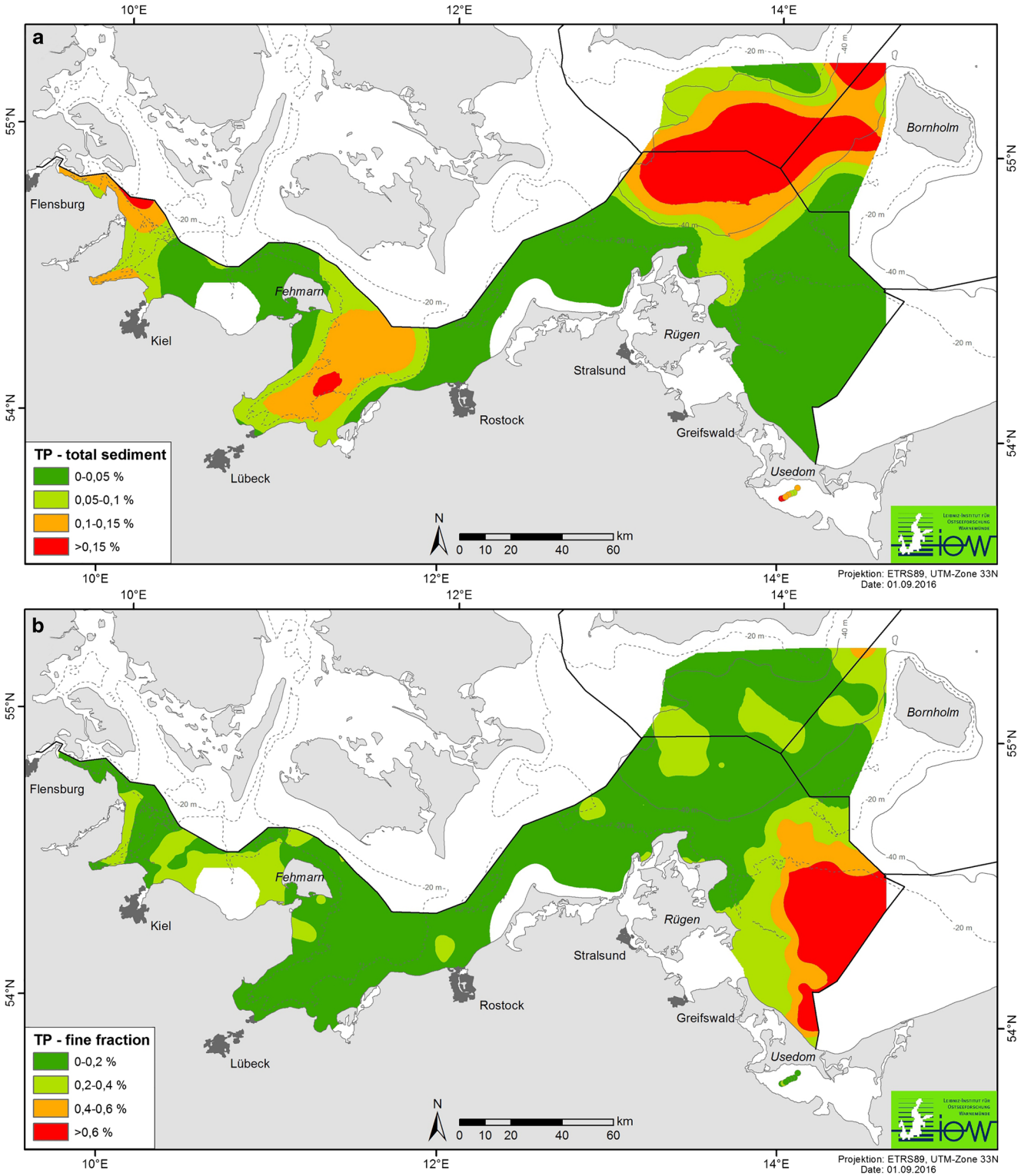

Fig. 5 Distribution of phosphorus (weight% P): **a** total sediment, **b** fine fraction. Note that the scales (legends) of the content ranges are different in **a** and **b**, which improves the visibility of the gradients

fraction for TOC (Fig. 4) and P (Fig. 5). For Hg (Fig. 6), the same scale was used. Some remarkable and partly unexpected distribution patterns are evident in the maps. Geochemically related elements show similar patterns, due to their dependency on material sources, pathways and cycles (see Discussion).

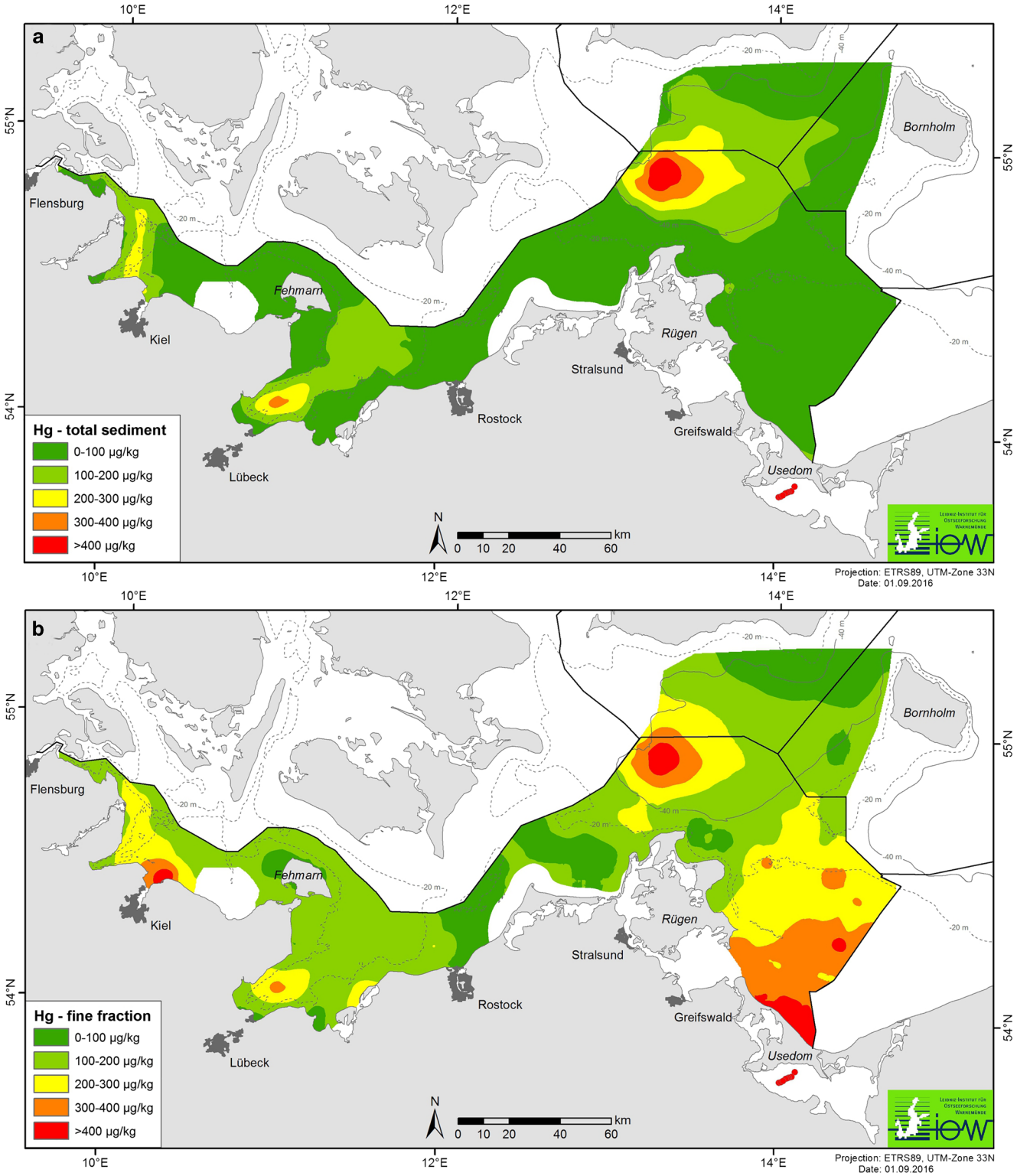

Fig. 6 Distribution of mercury (Hg, µg/kg): **a** total sediment, **b** fine fraction. Here **a** and **b** have the same scale (legends)

The correlation coefficients between the analysed elements (Table 4) supports these affinities. The correlation coefficients between most elements of similar properties and/or possible binding partners are highly positive. However, because the separation of the fine fraction is already a form of normalisation, the correlation coefficients are probably lower than expected. The coefficients obtained for total sediment contents (not shown) for all analysed elements are much higher (all

Table 3 Statistical parameters of sample analyses results (*n* number of samples)

Parameter	Component							
	<63 μm (%)	Hg (μg/kg)	N (%)	S (%)	TIC (%)	TOC (%)	TOC/N	Bio-opal (%)
n	867	859	856	764	836	856	853	796
Median	20.54	157	0.541	0.44	0.28	4.33	7.9	4.52
Mean	40.47	196	0.580	0.52	0.53	4.59	8.1	5.10
Min.	0.08	17	0.077	0.02	0.07	0.66	5.6	0.10
Max.	100	1,138	2.011	3.02	6.16	19.47	12.7	19.99
	As (mg/kg)	Cr (mg/kg)	Cu (mg/kg)	Fe (%)	Mn (mg/kg)	P (%)	Pb (mg/kg)	Zn (mg/kg)
n	573	602	602	602	602	602	602	602
Median	16.0	44.7	76.7	2.91	360	0.152	74.0	173.5
Mean	18.8	44.6	121.4	3.02	822	0.208	85.4	212.3
Min.	0.8	10.6	15.8	0.76	62	0.044	16.0	39.4
Max.	95.7	103.6	1,200	9.08	11,450	1.205	465	1,075

above 0.9), being a direct function of the grain-size effect. For general information about the geochemical composition of mud sediments of the Baltic Sea, see also Emelyanov (2012).

The regional distribution of organic carbon (TOC), which mainly reflects the primary production and deposition of young or fresh organic matter (TOC/N ratios mostly ranging between 7 and 9, see Table 3), is illustrated in Fig. 4. Comparing the distribution maps of TOC contents for the total sediment (Fig. 4a) and the fine fraction (Fig. 4b) with that of mud (Fig. 3), some striking differences are observed. The distribution of TOC in the total sediment mirrors that of mud, indicating that TOC contents increase with increasing mud content. The opposite is true for TOC in the fine fraction, where the highest contents occur in areas of low mud contents. Very similar patterns were found for nitrogen and biogenic opal (not shown here).

Similar patterns are observed for total P (Fig. 5). The highest contents of P in the total sediment are positively correlated with the mud distribution (Fig. 5a), whereas the fine-fraction distribution shows a markedly different pattern (Fig. 5b). This applies especially to the south-eastern part of the study area (Pomeranian Bight), but interestingly not to the central part where P is low in both the fine fraction and the total sediment. This general trend may be explained by the fact that P is partly mobile and therefore mainly bound to iron oxyhydroxide, which is redox-sensitive and can be mobilised by iron reduction due to organic matter degradation.

P geochemistry has been the focus of several studies during the past decade, especially for the Baltic Sea (e.g. Lukawska-Matuszewska and Bolalek 2008; Mort et al. 2010; Jilbert et al. 2011; Puttonen et al. 2014). Because it was not possible to analyse P binding forms by sequential extraction methods (SEDEX; Ruttenberg 1992) for all the samples of this study, a selected sample set (*n*=10) was analysed in a specialised laboratory in Utrecht, Holland. The SEDEX results are (given as averages in % rel. From total extracted P, which was 900 mg/kg dry weight): easily exchangeable P: 1.2%; Fe-bound P: 25%; authigenic Ca-P: 24%; detritic P: 24%; organically bound P: 26%. The easily exchangeable part is nevertheless important. Possible mobile

Table 4 Matrix of correlation coefficients for TOC, opal, and element contents in the sediment fine fraction

	TOC	Hg	Opal	As	Cr	Cu	Fe	Mn	P	Pb	Zn
TOC	1.00										
Hg	0.60	1.00									
Opal	0.52	0.45	1.00								
As	0.50	0.49	0.37	1.00							
Cr	0.65	0.56	0.54	0.62	1.00						
Cu	0.36	0.38	0.39	0.37	0.57	1.00					
Fe	0.57	0.48	0.42	0.77	0.82	0.45	1.00				
Mn	0.47	0.20	0.37	0.45	0.61	0.52	0.65	1.00			
P	0.54	0.40	0.42	0.52	0.65	0.62	0.63	0.67	1.00		
Pb	0.46	0.71	0.44	0.60	0.62	0.35	0.61	0.24	0.4	1.00	
Zn	0.50	0.66	0.44	0.62	0.69	0.56	0.64	0.45	0.50	0.73	1.00

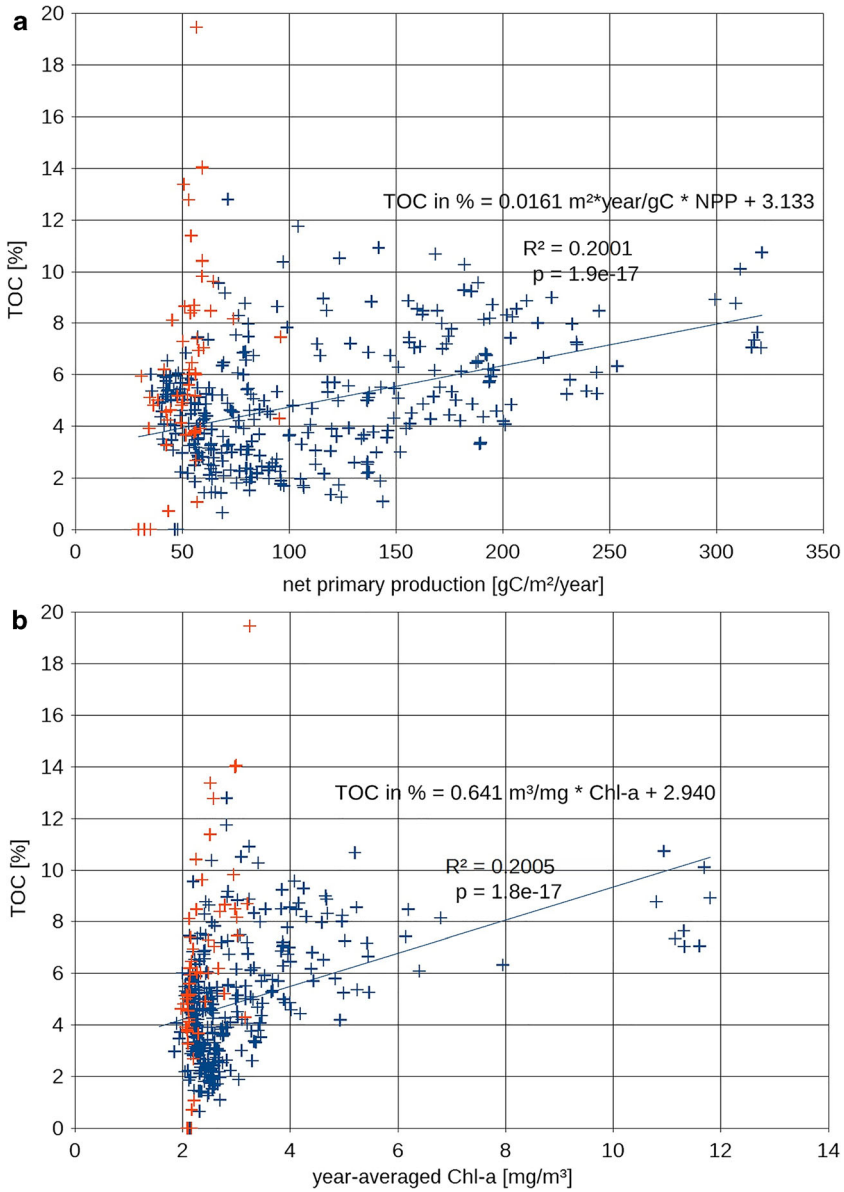

Fig. 7 Correlation of TOC content in the fine sediment fraction with **a** average net primary production derived from a numerical model for 2003, **b** chl-a concentration in the water column determined from satellite measurements (average of all validated measurements in the period 01 April 2015 to 01 April 2016)

P, driven by changing environmental conditions (e.g. redox), is the Fe-bound portion if sedimentary conditions switch from oxic to anoxic, with a smaller contribution from degradation of organic matter (organically bound P). This means that about ¼ of the total P in the sediments could be mobilised by short-term changes at the sediment surface. Longer-term changes—e.g. early diagenetic reactions or further mineralisation of organic matter in deeper sediment layers—should lead to strong changes in the different binding forms and the related concentrations or contents in the sediments. This, and additional pore-water measurements, are subject of ongoing and future investigations in the present study area. The strongly varying nature of bottom oxygen concentrations was recently summarised for the study area by Zettler et al. (2017).

In contrast to TOC and P, the distribution pattern of mercury (Hg) shows a more complex pattern (Fig. 6). Similarly to the former two constituents, Hg is positively related to mud content in the total sediment, although restricted to more confined areas (Fig. 6a). In the case of the mud fraction, Hg is partly positively and partly negatively related to mud content, depending on the location in the study area (Fig. 6b). The negative relation is particularly prominent in the southern Pomeranian Bight. This more complex distribution pattern of Hg can be explained by it being mainly an anthropogenic pollutant. Other anthropogenic sourced heavy metals and As (not shown here) are characterised by similar distribution patterns. Particularly, historical hotspots (dumping sites) are seen in the western Arkona Basin and the inner part of Mecklenburg Bay. For the sandy area of the Oder Bank and

Pomeranian Bight, the impact of (old) polluted material from the Oder estuary is visible (see also Discussion).

Model results

The TOC content of the fine fraction (Fig. 4b) shows highest values in the Oder Lagoon and Pomeranian Bight. To assess whether these values originate from high local primary production, TOC was correlated with modelled primary production (Fig. 7a) and measured chl-a values (Fig. 7b). The comparison is restricted to a longitudinal corridor between 13.5°E and 14.3°E (blue crosses in Fig. 7) to characterise the transitional area between the Oder Bank and the Arkona Basin. Values east of 14.3°E are shown in orange to highlight the data from the shallow Oder Bank.

The comparison with both measured chl-a and modelled net primary production (NPP) shows essentially the same trend, but with low correlation. Whereas high local NPP is associated with elevated TOC contents in the fine fraction, the reverse is not always the case, i.e. in low-productivity areas the TOC contents can be high or low. High TOC contents can be observed even in areas of relatively low NPP.

Discussion

For further interpretation of the present results, it is necessary to first consider the relations between freshly deposited material, often called "fluffy layer", and the 2 cm surface sediment samples used for this study. This concerns the age or time span represented in the analysed material, and possible impacts related to temporal variability and various sediment mixing processes. The fluffy layer likely results from primary production but is also affected by re-suspended and re-deposited (older) material from lateral transport driven by intensive hydrodynamics. For the eastern part of the study area, this has been investigated by Löffler et al. (2000), Kuhrts et al. (2004), and Tauber and Emeis (2005). Dating by radio-nuclides (e.g. ^{210}Pb, ^{137}Cs) is rather difficult or impossible even in the mud-filled basins of the study area (see Leipe et al. 2013; Moros et al. 2017). The 2 cm sediment surface samples would contain the fluffy layer material plus older material mixed by bioturbation, hydro-turbation and direct anthropogenic impact (ground fishery). This concerns both the fine-grained muddy sediments of the basins as well as the sands of the shallower banks.

There seems to be no way to restrict the time span to specific years or to separate what portion is old and what is young material. Therefore, the element maps shown in Figs. 4, 5 and 6 likely represent the average state resulting from variable depositional conditions of the past decades.

Kersten et al. (2005) used the short-life ^{234}Th isotope for investigating storm-driven disturbances and transport in muddy sediments of the Mecklenburg Bight, and found a large area impacted by an old dumping site of contaminated material. For this example and the present study, the anthropogenically sourced impact/input of heavy metals (e.g. Hg) can be used as tracer for the reconstruction of transport pathways, and the time span is restricted by the pollution history. The deeper, mud-filled basins in the present study area can be regarded as depositional sites (albeit not undisturbed) in comparison to the sandy banks and coastal zones where the fine-fraction content is lower and the hydrodynamics is stronger.

The grain-size effect

A general comparison of the two maps (total sediment and fine fraction) for each of the elements discussed here shows evidence of the so-called grain-size effect. According to the expected transport energy, the fine-grained material (as major carrier of these elements) mainly deposits in the basins, whereas the coarser sediments (sands) of the shallower banks and coastal zones are depleted in fine-grained material. This simple sorting is driven by decreasing energy, but not necessarily leading to differences of element contents *inside* the fine fraction for areas of high or low proportions of this fine fraction. Indeed, in the present case local geochemical "anomalies" can plausibly be explained rather in terms of point source or concentration/enrichment effects rooted in chemical and/or biological reactions (see below).

Nutrients, productivity, benthic fauna

The eastern part of the study area, the Pomeranian Bight with the sand-covered Oder Bank in its centre, is a good example of a highly productive sector. In the south, the Oder River estuary represents an important source for nutrients (Voss and Struck 1997) and pollutants. The whole bight is characterised by high primary production from spring to autumn, besides being densely colonised by benthic organisms (Glockzin and Zettler 2008). At least three important species of benthic macrofauna (*Mya arenaria*, *Macoma balthica*, *Cerastoderma glaucum*) are present with remarkably high biomasses in sandy areas (Darr et al. 2014). The nutrient chain, starting from primary production (e.g. diatoms) to filter-feeding bivalves and eventually predators, is short (cf. shallow waters) and very intense. Huge flocks of sea-ducks overwinter in this internationally recognised bird resting site, feeding mainly on benthic macrofauna (Kube 1996).

The Pomeranian Bight and Oder Bank constitute a hotspot for biogeochemical material cycling. However, the bight is not a (long-term) depositional area for fine-grained material. Organic matter and fine particle-bound nutrients and pollutants are transported towards the adjacent basins (Arkona Basin, Bornholm Basin). Due to the high energy input, strong re-suspension occurs and the residence time for fluffy layer material has been estimated to be in the range of weeks to

months (Christiansen et al. 2002; Emeis et al. 2002; Kuhrts et al. 2004). Nevertheless, some of the fine fraction in this sandy area is remarkably enriched in organic carbon and nutrients (P, bio-SiO_2).

The correlation of TOC in the fine fraction with chl-a and net primary production (Fig. 7), however, shows that high local TOC contents do not necessarily originate from local production. While high local productivity values always correspond to TOC enrichment in the fine fraction, the opposite is not true, high TOC values being found also in the easternmost part of the Oder Bank. In this relatively exposed area, chl-a values and primary productivity are much lower compared to the immediate proximity of the coast or even the Oder Lagoon. One possible explanation could be lateral transport processes, the fine fraction deposited here possibly originating from even more heavily euthrophied sites close to the Oder River mouth from where it is transported by repeated sedimentation and re-suspension. The high Hg content in this area (Fig. 6b) supports this hypothesis. Nevertheless, the real causes of element enrichment in the fine sediment fraction of the shallow Oder Bank remain unclear. Probably the geochemical function of benthic fauna (e.g. filter feeders) is more important than one would suppose but this needs confirmation in further investigations (see also Gogina et al. 2017).

Pollution

Mercury (Hg) can be used as a strong indicator for anthropogenically sourced environmental pollution (Fig. 6). Two historical hotspots are clearly visible in both Hg distribution maps. The industrial waste dumping site in the Mecklenburg Bight dates back to the 1960s, and the hotspot in the Arkona Basin reflects post-World War II dumping activities. Both are situated in mud-filled basins and have already been pinpointed during former investigations (see Leipe et al. 2013). An interesting new result is that the distribution of Hg in the fine fraction of southern Pomeranian Bight sediments (Fig. 6b) reveals the ongoing transport of (old) contaminated material from the Oder Lagoon to the open Baltic Sea. The soft sediments of the Oder Lagoon act as a stopover of pollutants (and nutrients) from historical times when pollution of the river was at its maximum (ca. 1960–1990; see Leipe et al. 1998). It is mainly the wind-driven re-suspension of the surface sediment in the shallow lagoon (average depth 3.8 m) which regularly leads to material transport with the river discharge into the open Baltic Sea (Tejakusuma 2004).

Beldowski and Pempkowiak (2003) found similar results for the Gdansk Basin, Vistula River mouth region in Poland, with a transport chain from the river (source) to the depositional basins. They observed an additional impact of (chemical) remobilisation caused by changes in speciation of Hg, which could not be determined in the present study. An impoverishment or decreasing trend of Hg contents with increasing distance from hotspots or sources (chemical aureole) is clearly visible in the fine-fraction Hg map. However, a general decrease of pollution over, for example, the past two decades can be reconstructed only in well-dated undisturbed sediment cores (see Moros et al. 2017, and comments above). Elevated Hg contents have also been recorded in Kiel Bay, indicating contamination by local industry and harbour activities.

Conclusions

Further investigations should focus on estimating volume-related element concentrations (see Flemming and Delafontaine 2000, 2016; Leipe et al. 2011) considering sediment water content and dry bulk density based on the results of this study. This would allow to determine inventories and even accumulation rates, if dating is possible for selected sediment cores from the sub-areas discussed here. Questions related to material cycles and diagenetic processes would furthermore require the analyses of pore-water profiles and element speciation for P, Ca, Fe and trace metals (e.g. Hg; see Beldowski and Pempkowiak 2003, 2007).

For geochemical investigations of large areas with a heterogeneous sediment distribution, a separation of the fine fraction before analyses (similar to monitoring programs) is recommended and offers several advantages. The grain-size effect ("dilution" by sand) can be excluded and, additionally, geochemical "anomalies" become visible. In the present study area in the south-western Baltic Sea, the data reveal local hotspots of, for example, Hg of mainly anthropogenic origin (dumping sites, river discharge). Furthermore, and rather unexpectedly, there are enrichments of TOC and elements (e.g. P) in shallow-water areas (sandbanks) which could be related to local conditions involving, for example, dense benthic fauna or biogeochemical reactions at the sediment–water interface. The distribution of local or sub-regional primary production alone could not be confirmed as the main source. For further investigations of material sources, pathways and cycles, the deposition of biogeochemical and environmentally relevant elements, as well as (volume related) concentration-based maps, the presented examples of element maps are the first step. Including the original data behind these maps, modern web-GIS portals are surely the future of inter- and multidisciplinary science and a powerful interface for public use.

Acknowledgements We acknowledge the provision of weather forecast data from the German Weather Service (DWD) and the kind assistance with laboratory work by Ines Scherff, Sibylle Fink, Anke Bender and Anne Köhler. Special thanks go to Prof. Caroline Slomp, Utrecht, Holland, for analyses of P speciation in a selected set of our samples. We are grateful to the reviewers and the editors for constructive and critical comments. The SECOS project was funded by the German Federal Ministry of Education and

Research (http://bio-50.io-warnemuende.de/secos/). RF was partly funded by the German Federal Ministry for Education and Research in the KÜNO Project MOSSCO (03F0740B), and by the BONUS-BaltCoast project (03F0717A). Supercomputing power was provided by HLRN (North-German Supercomputing Alliance).

Compliance with ethical standards

Conflict of interest The authors declare that there is no conflict of interest with third parties.

References

Beldowski J, Pempkowiak J (2003) Horizontal and vertical variabilities of mercury concentration and speciation in sediments of the Gdansk Basin, southern Baltic Sea. Chemosphere 52:645–654

Beldowski J, Pempkowiak J (2007) Mercury transformations in marine coastal sediments as derived from mercury concentration and speciation changes along source/sink transport pathway (southern Baltic). Estuarine, Coastal and Shelf Science 72:370–378

Borg H, Jonsson P (1996) Large-scale metal distribution in Baltic Sea sediments. Marine Pollution Bulletin 32:8–21

Bruggeman J, Bolding K (2014) A general framework for aquatic biogeochemical models. Environmental Modelling and Software 61: 249–265

Burchard H, Bolding K (2002) GETM—A general estuarine transport model. Scientific documentation, tech Rept EUR 20253 EN

Christiansen C, Edelvang K, Emeis K-C, Graf G, Jähmlich S, Kozuch J, Laima M, Leipe T, Löffler A, Lund-Hansen L-C, Miltner A, Pazdro K, Pempkowiak J, Shimmield G, Shimmield T, Smith J, Voss M, Witt G (2002) Material transport from the nearshore to the basinal environment in the southern Baltic Sea, I: processes and mass estimates. Journal of Marine Systems 35:133–150

Conley DJ (1998) An interlaboratory comparison for the measurement of biogenic silica in sediments. Marine Chemistry 63:39–48

Darr A, Gogina M, Zettler ML (2014) Detecting hot-spots of bivalve biomass in the south-western Baltic Sea. Journal of Marine Systems 134:69–80

Doerffer R (2014) Algorithm theoretical bases document (ATBD) for L2 processing of MERIS data of case 2 waters, 4th reprocessing. ESA 20140825, MERIS ATBD 2.312

Emeis K-C, Christiansen C, Edelvang K, Jähmlich S, Kozuch J, Laima M, Leipe T, Lund-Hansen L-C, Löffler A, Miltner A, Pazdro K, Pempkowiak J, Pollehne F, Shimmield T, Voss M, Witt G (2002) Material transport from the nearshore to the basinal environment in the southern Baltic Sea, II: synthesis of data on origin and properties of material. Journal of Marine Systems 35:151–168

Emelyanov EM (ed) (2002) Geology of the Gdansk Basin, Baltic Sea. Russian Academy of Sciences, Shirshov Institute of Oceanology, Kaliningrad, Russia

Emelyanov EM (2012) The distribution of organic carbon and composition of the carboniferous mud in the Baltic Sea. Adv Environm Res 27:111–138

Emelyanov E, Christiansen C, Michelsen O (eds) (1995) Geology of the Bornholm Basin. Aarhus University, Aarhus, Denmark, Department of Earth Sciences

Flemming BW, Delafontaine MT (2000) Mass physical properties of muddy intertidal sediments: some applications, misapplications and non-applications. Continental Shelf Research 20:1179–1197

Flemming BW, Delafontaine MT (2016) Mass physical sediment properties. In: Kennish MJ (ed) Encyclopedia of estuaries. Springer, Dordrecht, pp 419–432. doi:10.1007/978-94-017-8801-4_350

Glockzin M, Zettler ML (2008) Spatial macrozoobenthic distribution patterns in relation to major environmental factors – a case study from the Pomeranian Bay (southern Baltic Sea). Journal of Sea Research 59:144–161

Gogina M, Morys C, Forster S, Gräwe U, Friedland R, Zettler ML (2017) Towards benthic ecosystem functioning maps: quantifying bioturbation potential in the German part of the Baltic Sea. Ecological Indicators 73:574–588. doi:10.1016/j.ecolind.2016.10.025

Gräwe U, Naumann M, Mohrholz V, Burchard H (2015a) Anatomizing one of the largest saltwater inflows into the Baltic Sea in December 2014. Journal of Geophysical Research, Oceans 120:7676–7697. doi:10.1002/2015JC011269

Gräwe U, Holtermann P, Klingbeil K, Burchard H (2015b) Advantages of vertically adaptive coordinates in numerical models of stratified shelf seas. Ocean Modell 92:56–68. doi:10.1016/j.ocemod.2015.05.008

HELCOM (2007) Baltic Sea Action Plan. HELCOM Extraordinary Ministerial Meeting, 15 November 2007, Krakow, Poland

HELCOM (2015) Updated fifth Baltic Sea pollution load compilation (PLC-5.5). Baltic Sea environment proceedings no 145. Helsinki commission, Helsinki, Finland

Hofmeister R, Burchard H, Beckers J-M (2010) Non-uniform adaptive vertical grids for 3D numerical ocean models. Ocean Modell 33:70–86. doi:10.1016/j.ocemod.2009.12.00313

Jilbert T, Slomp CP, Gustafsson BG, Boer W (2011) Beyond the Fe-P-redox connection: preferential regeneration of phosphorus from organic matter as a key control on Baltic Sea nutrient cycles. Biogeosciences 8:1699–1720

Kersten M, Leipe T, Tauber F (2005) Storm disturbance of sediment contaminants at a hot-spot in the Baltic Sea assessed by ^{234}Th radionuclide tracer profiles. Environmental Science & Technology 39: 984–990

Klingbeil K, Burchard H (2013) Implementation of a direct nonhydrostatic pressure gradient discretisation into a layered ocean model. Ocean Modell 65:64–77. doi:10.1016/j.ocemod.2013.02.002

Klingbeil K, Mohammadi-Aragh M, Gräwe U, Burchard H (2014) Quantification of spurious dissipation and mixing – discrete variance decay in a finite-volume framework. Ocean Modell 81:49–64. doi:10.1016/j.ocemod.2014.06.001

Kube J (1996) The ecology of macrozoobenthos and sea ducks in the Pomeranian Bay. Institute of Baltic Sea Research, Warnemünde, Marine Science Reports no 18

Kuhrts C, Fennel W, Seifert T (2004) Model studies of transport of sedimentary material in the western Baltic. Journal of Marine Systems 52:167–190

Lääne A, Pitkänen H, Arheimer B, Behrendt H, Jarosinski W, Sarmite L, Pachel K, Shekhovtsov A, Svendsen LM, Valatka S (2002) Evaluation of the implementation of the 1988 ministerial declaration regarding nutrient load reductions in the Baltic Sea catchment area. Finnish Marine Research 247:38–50

Leipe T, Eidam J, Lampe R, Meyer H, Neumann T, Osadczuk A, Janke W, Puff T, Blanz T, Gingele FX, Dannenberger D, Witt G (1998) The Oder-lagoon, contributions to Holocene development and anthropogenic impact of the Oder estuary (in German). Institute of Baltic Sea Research, Warnemünde, Marine Science Reports no 28

Leipe T, Tauber F, Vallius H, Virtasalo J, Uścinowicz S, Kowalski N, Hille S, Lindgren S, Myllyvirta T (2011) Particulate organic carbon (POC) in surface sediments of the Baltic Sea. Geo-Marine Letters 31:175–188. doi:10.1007/s00367-010-0223-x

Leipe T, Moros M, Kotilainen A, Vallius H, Kabel K, Endler M, Kowalski N (2013) Mercury in Baltic Sea sediments – natural background and anthropogenic impact. Chemie Erde (Geochemistry) 73: 249–259

Löffler A, Leipe T, Emeis KC (2000) The "fluffy layer" in the Pomeranian bight (western Baltic Sea): geochemistry, mineralogy and environmental aspects. Meyniana 52:85–100

Lukawska-Matuszewska K, Bolalek J (2008) Spatial distribution of phosphorus forms in sediments in the Gulf of Gdansk (southern Baltic Sea). Continental Shelf Research 28:977–990

Moros M, Andersen TJ, Schulz-Bull D, Häusler K, Bunke D, Snowball I, Kotilainen A, Zillen L, Jensen JB, Kabel K, Hand I, Leipe T, Lougheed BC, Wagner B, Arz HW (2017) Towards an event stratigraphy for Baltic Sea sediments deposited since AD 1900: approaches and challenges. Boreas 46:129–142

Mort HP, Slomp CP, Gustafsson BG, Andersen TJ (2010) Phosphorus recycling and burial in Baltic Sea sediments with contrasting redox conditions. Geochimica et Cosmochimica Acta 74:1350–1362

Müller PJ, Schneider R (1993) An automated leaching method for the determination of opal in sediments and particulate matter. Deep-Sea Research Part I 40(3):425–444

Pitarch J, Volpe G, Colella S, Krasemann H, Santoleri R (2016) Remote sensing of chlorophyll in the Baltic Sea at basin scale from 1997 to 2012 using merged multi-sensor data. Ocean Science 12:379–389. doi:10.5194/os-12-379-2016

Puttonen I, Mattila J, Jonsson P, Karlsson OM, Kohonen T, Kotilainen A, Lukkari K, Malmaeus JM, Rydin E (2014) Distribution and estimated release of sediment phosphorus in the northern Baltic Sea archipelagos. Estuarine, Coastal and Shelf Science 145:9–21

Radtke H, Neumann T, Voss M, Fennel W (2012) Modeling pathways of riverine nitrogen and phosphorus in the Baltic Sea. Journal of Geophysical Research, Oceans 117(C9):2156–2202. doi:10.1029/2012JC008119

Ruttenberg KC (1992) Development of a sequential extraction method for different forms of phosphorus in marine sediments. Limnology and Oceanography 37:1460–1482

Tauber F (2012) Seabed sediments in the German Baltic Sea (in German). 9 map sheets. Bundesamt für Seeschifffahrt und Hydrographie, Hamburg-Rostock

Tauber F, Emeis K-C (2005) Sediment mobility in the Pomeranian bight (Baltic Sea): a case study based on sidescan-sonar images and hydrodynamic modeling. Geo-Marine Letters 25:221–229

Tejakusuma IG (2004) Investigations into the hydrography and dynamics of suspended particulate matter and sediments in the Oder Lagoon, southern Baltic Sea. PhD Thesis, University of Greifswald, Greifswald

Uscinowicz S (ed) (2011) Geochemistry of Baltic Sea surface sediments. Polish Geological Institute & Ministry of the Environment, Warsaw

Vallius H (ed) (2007) Holocene sedimentary environment and sediment geochemistry of the eastern Gulf of Finland, Baltic Sea. Geological Survey of Finland, Special Paper 45

Voss M, Struck U (1997) Stable nitrogen and carbon isotopes as indicator of eutrophication of the Oder River (Baltic Sea). Marine Chemistry 59:35–49

Zettler ML, Friedland R, Gogina M, Darr A (2017) Variation in benthic long-term data of transitional waters: is interpretation more than speculation? PloS One 12(4):e0175746. doi:10.1371/journal.pone.0175746